CDDpress

www.nature.com/cddiscovery

ARTICLE OPEN

Check for updates

Altered muscle niche contributes to myogenic deficit in the D2-*mdx* model of severe DMD

Davi A. G. Mázala[1,2,6], Ravi Hindupur[1,6], Young Jae Moon[1,3], Fatima Shaikh[1], Iteoluwakishi H. Gamu[1], Dhruv Alladi[1], Georgiana Panci[4], Michèle Weiss-Gayet[4], Bénédicte Chazaud[4], Terence A. Partridge[1,5], James S. Novak[1,5]✉ and Jyoti K. Jaiswal[1,5]✉

Lack of dystrophin expression is the underlying genetic basis for Duchenne muscular dystrophy (DMD). However, disease severity varies between patients, based on specific genetic modifiers. D2-*mdx* is a model for severe DMD that exhibits exacerbated muscle degeneration and failure to regenerate even in the juvenile stage of the disease. We show that poor regeneration of juvenile D2-*mdx* muscles is associated with an enhanced inflammatory response to muscle damage that fails to resolve efficiently and supports the excessive accumulation of fibroadipogenic progenitors (FAPs), leading to increased fibrosis. Unexpectedly, the extent of damage and degeneration in juvenile D2-*mdx* muscle is significantly reduced in adults, and is associated with the restoration of the inflammatory and FAP responses to muscle injury. These improvements enhance regenerative myogenesis in the adult D2-*mdx* muscle, reaching levels comparable to the milder B10-*mdx* model of DMD. Ex vivo co-culture of healthy satellite cells (SCs) with juvenile D2-*mdx* FAPs reduces their fusion efficacy. Wild-type juvenile D2 mice also manifest regenerative myogenic deficit and glucocorticoid treatment improves their muscle regeneration. Our findings indicate that aberrant stromal cell responses contribute to poor regenerative myogenesis and greater muscle degeneration in juvenile D2-*mdx* muscles and reversal of this reduces pathology in adult D2-*mdx* muscle, identifying these responses as a potential therapeutic target for the treatment of DMD.

Cell Death Discovery (2023)9:224 ; https://doi.org/10.1038/s41420-023-01503-0

INTRODUCTION

Duchenne muscular dystrophy (DMD) is a progressive X-linked myopathy caused by mutations that prevent the expression of dystrophin—the muscle structural protein that links myofibrillar actin and the extracellular matrix (ECM) [1–4]. Lack of dystrophin makes the myofiber sarcolemma susceptible to injury and compromises sarcolemmal repair, causing asynchronous myofiber damage and chronic inflammation [5–8]. Muscles from DMD patients and animal models display chronic inflammation, ECM remodeling, fibro-fatty replacement, and progressive muscle loss that diminishes muscle function [9–12]. Additionally, there is evidence of progressive reduction of satellite cells (SC) and their myogenic capacity due to constant muscle injury and turnover, which leads to greater myofiber loss and replacement by fibrotic tissue in DMD patients [13, 14]. Chronic inflammation and ECM degradation also alter the muscle niche that supports SC function, while genetic modifiers that affect ECM remodeling alter disease severity in DMD patients [15–17].

One of the genetic modifiers of DMD is the polymorphism in latent transforming growth factor binding protein 4 (LTBP4) that diminishes the sequestration of transforming growth factor β (TGF-β) in its latent state [18]. Mice of the DBA/2J (D2) background carries a LTBP4 allele that fails to keep TGF-β in its latent state, leading to its heightened activation [19, 20]. D2 mice that also lack dystrophin (D2-*mdx*) mimic the severity of disease observed in DMD patients [19–24]. TGF-β modulates dynamic interactions of macrophages, SCs, and other muscle interstitial cell types during healthy muscle regeneration [25–29]. Heightened TGF-β activity disrupts the muscle extracellular niche by altering the crosstalk between stromal cells, including inflammatory cells such as macrophages, and fibroadipogenic progenitors (FAPs), whose interactions support regenerative myogenesis [30–32]. Disruption of macrophage and FAP interactions in damaged muscle delays FAP clearance and promotes fibrosis that further impairs regenerative myogenesis [29, 30, 33–36]. Chronic inflammation due to recurrent injury disrupts the synchrony of stromal cell communication required for successful muscle repair [6, 8, 33]. The impact of asynchronous muscle reparative response is demonstrated by failed muscle regeneration and fibroadipogenic muscle loss provoked by repeated muscle injury in a milder model of DMD [8, 34]. Muscle damage due to spontaneous activity-driven muscle contraction (spontaneous injury) in the severe juvenile D2-*mdx* model is associated with increased degeneration and failed regeneration [20, 23, 24].

Here, we demonstrate that the severe muscle damage and myogenic failure observed in juvenile D2-*mdx* is unexpectedly

[1]Center for Genetic Medicine Research, Children's National Research Institute, Children's National Hospital, Washington, DC 20012, USA. [2]Department of Kinesiology, College of Health Professions, Towson University, Towson, MD 21252, USA. [3]Department of Biochemistry and Orthopaedic Surgery, Jeonbuk National University Medical School and Hospital, Jeonju 54907, Republic of Korea. [4]Institut NeuroMyoGène, Unité Physiopathologie et Génétique du Neurone et du Muscle, INSERM U1513, CNRS UMR 5261, Université Claude Bernard Lyon 1, Univ Lyon, Lyon, France. [5]Departments of Pediatrics and Genomics and Precision Medicine, The George Washington University School of Medicine and Health Sciences, Washington, DC 20052, USA. [6]These authors contributed equally: Davi A. G. Mázala, Ravi Hindupur. ✉email: jnovak@childrensnational.org; jkjaiswal@cnmc.org

Received: 31 January 2023 Revised: 6 June 2023 Accepted: 19 June 2023
Published online: 04 July 2023

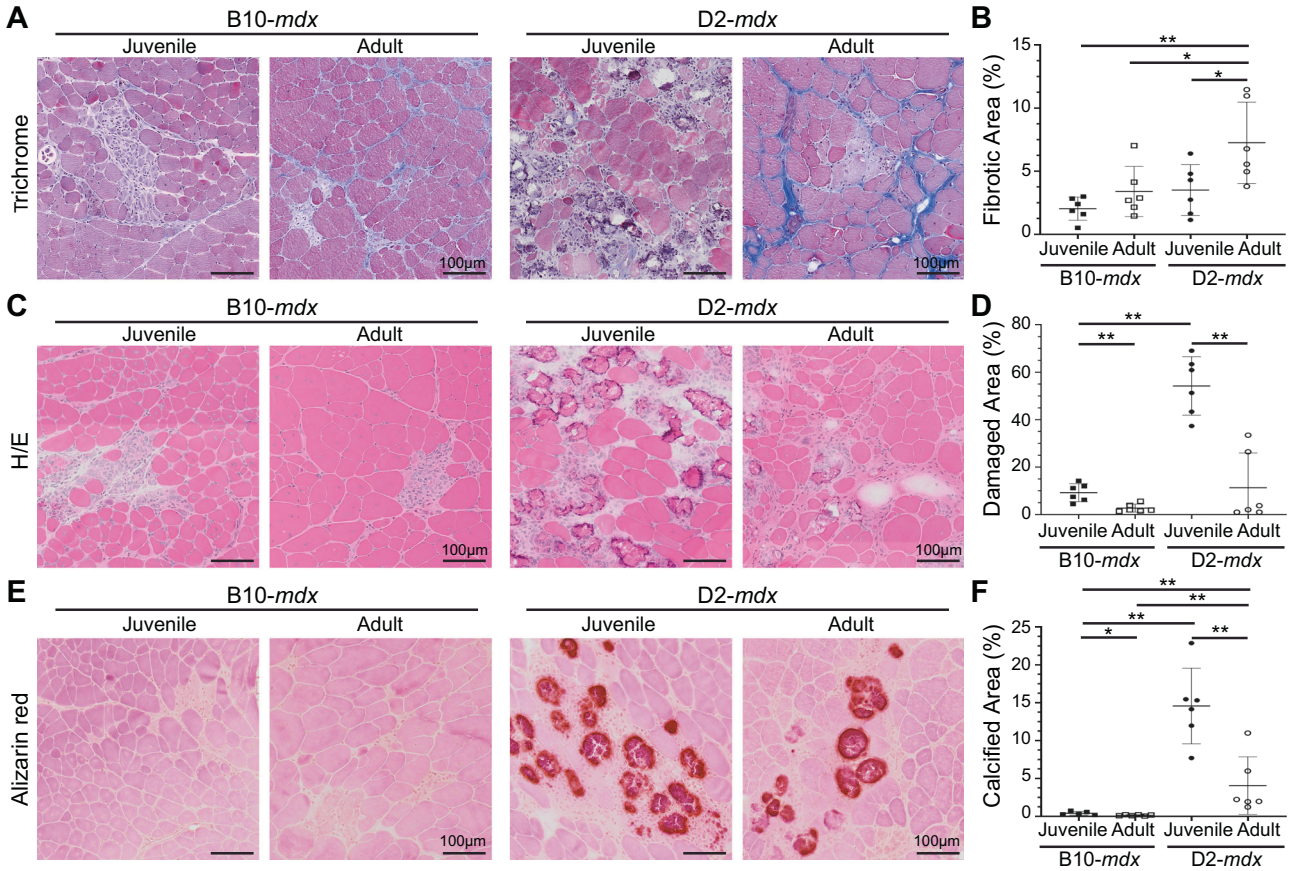

Fig. 1 Histopathological assessment of disease in D2-*mdx* and B10-*mdx* models. A, **B** Masson's trichrome staining and quantification of percent fibrotic tissue area performed on triceps harvested from juvenile (5.5 ± 1.5 wk) and adult (8.5 ± 1.5 mo) D2-*mdx* and B10-*mdx* mice. **C**, **D**. H&E staining and quantification of percent damaged muscle tissue area performed on triceps harvested from juvenile and adult D2-*mdx* and B10-*mdx* mice; damaged areas were characterized by the presence of interstitial mononuclear cells, damaged myofibers, and appearance of small-diameter centrally nucleated fibers (CNFs). **E**, **F** Alizarin red staining and quantification of percent calcified fiber area performed on triceps harvested from juvenile and adult D2-*mdx* and B10-*mdx* mice. Data represent mean ± SD from $n = 6$ mice per cohort. *$p < 0.05$, **$p < 0.01$ by Mann–Whitney test. Refer to Supplementary Fig. 1.

improved in muscles from adult D2-*mdx* mice. We performed a comparative analysis of muscle histopathological changes in the adult versus the juvenile D2-*mdx* and examined the underlying mechanism for this difference in disease severity between adult and juvenile D2-*mdx*. This investigation ascribes unresolved damage in juvenile D2-*mdx* muscle to excessive inflammatory and fibroadipogenic responses, restoration of which in adult muscle improves regenerative myogenesis. Using in vivo injury and ex vivo SC and FAP co-cultures, we show that these aberrant stromal interactions drive myogenic deficit in D2-*mdx* muscles and establish the importance of the muscle niche in the regenerative deficit and disease severity in DMD.

RESULTS

Juvenile D2-mdx mice exhibit excessive muscle damage

We have previously described the sudden onset of histological damage, and rapid disease progression in muscles of juvenile (~5 wk) D2-*mdx* [20], and reported triceps as among the most severely affected muscles in this model [20]. Consistent with other reports in adult D2-*mdx* [19, 21–23], we observed extensive networks of endomysial and perimysial fibrosis in the triceps of adult (>7 months old) D2-*mdx* (Fig. 1A, B). The interstitial fibrosis nearly doubled between juvenile and adult D2-*mdx* muscles, while only a modest increase was observed between juvenile and adult C57BL/10ScSn-mdx/J (B10-*mdx*) muscles (Fig. 1A, B). Despite the large increase in fibrosis in adult D2-*mdx* triceps, macroscopic examination revealed unexpected improvements in pathological features, prompting a detailed histological examination. H&E staining showed reduced spontaneous myofiber damage and fewer infiltrating mononuclear cells in adult D2-*mdx* than in juvenile D2-*mdx*, to levels comparable to the B10-*mdx* muscles (Fig. 1C, D, Supplementary Fig. 1). Alizarin red staining identified a notable decrease in areas of myofiber damage and calcified replacement from ~15% in juvenile D2-*mdx* to <5% in adult D2-*mdx* (Fig. 1E, F). Overall, our analysis revealed that while there is progressive increase in endomysial fibrosis from juvenile to adult D2-*mdx*, surprisingly the extent of damage in the adult D2-*mdx* is reduced, as compared to the juvenile D2-*mdx*, to levels observed in either juvenile or adult B10-*mdx*.

Juvenile D2-mdx muscle exhibits a regenerative deficit that is reversed in adult muscle

When assessing the adult D2-*mdx* histopathology relative to the juvenile D2-*mdx*, we observed a notable increase in the frequency of centrally nucleated fibers (CNFs) (Fig. 1C). Quantifying myofibers with internal nuclei as a percentage of total myofibers per cross-section revealed nearly 3-times more CNFs in adult D2-*mdx* as compared to juvenile D2-*mdx* (Fig. 2A, B). Consequently, while juvenile D2-*mdx* have fivefold fewer CNFs than juvenile B10-*mdx*, this difference is only twofold between the adult D2-*mdx* and B10-*mdx* (Fig. 2A, B). As juvenile D2-*mdx* muscles show minimal regenerative ability [20, 22, 24], we examined if regenerative capacity improved in adult D2-*mdx* muscle, leading to the

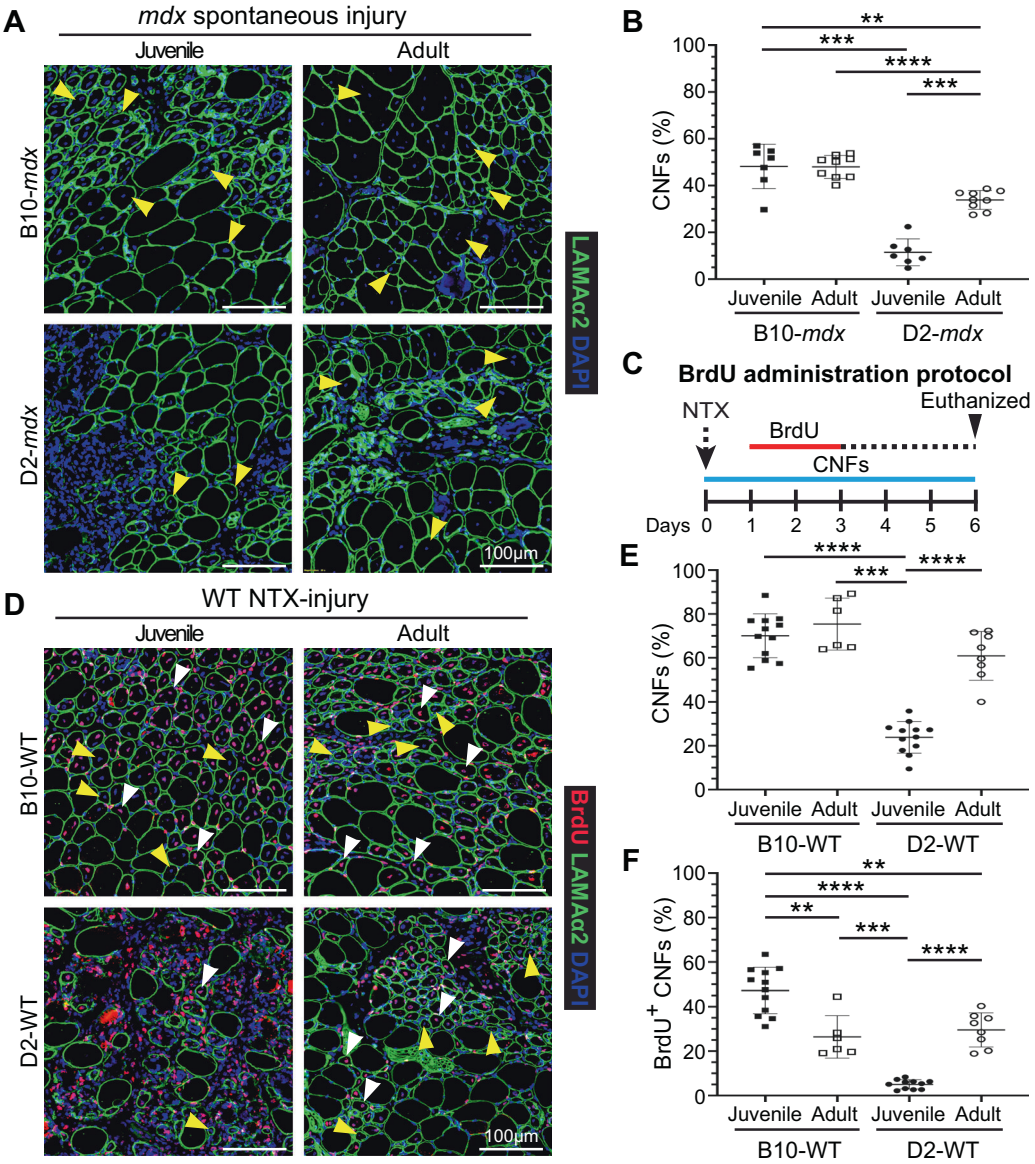

Fig. 2 Assessment of muscle regeneration in juvenile and adult *mdx* and WT mice. A IF images from juvenile (5.5 ± 1.5 wk) and adult (6.5 ± 1 mo) triceps muscle sections from dystrophic *mdx* mice stained to identify muscle fibers (Laminin-α2) and CNFs (DAPI). Yellow arrowheads show CNFs. **B** Quantification of CNFs from dystrophic triceps expressed as a percentage of total muscle fibers. **C** Schematic showing the BrdU 'myofiber birth dating' strategy to label proliferating SCs in NTX-injured TA muscles in juvenile (5.5 ± 1.5 wk) and adult (10.5 ± 0.5 mo) WT mice by BrdU administration from 24 to 72 h post injury (*green line*). Mice were euthanized and tissues were harvested 6 d post-injury. **D** IF images and quantification of muscle sections from B10-WT and D2-WT TA muscles stained to identify muscle fibers $BrdU^+$ CNFs and total CNFs; sections co-stained with Laminin-α2 and DAPI. White arrowheads show $BrdU^+$ CNFs while yellow arrowheads show CNFs. **E** Quantification of CNFs (%) from NTX-injured TA muscles harvested from juvenile and adult B10-WT and D2-WT mice harvested 6 dpi. **F** Quantification of $BrdU^+$ CNFs (%) from juvenile and adult B10-WT and D2-WT NTX-injured TA muscles. Data represent mean ± SD from $n = 7–9$ mice per cohort (**B**) or $n = 6–12$ NTX-injured TA muscles per cohort (**E**, **F**). $^*p < 0.05$, $^{**}p < 0.01$, $^{***}p < 0.001$, $^{****}p < 0.0001$ by Mann–Whitney test.

observed reduction in histopathology (Fig. 1). To investigate whether the earlier myogenic deficit in D2-*mdx* is rescued in adulthood, we used notexin (NTX) to acutely injure the tibialis anterior (TA) muscle of D2 wild-type (D2-WT) to avoid confounding effects of chronic and spontaneously-triggered muscle injury in D2-*mdx*. To monitor regenerative myogenesis that follows this acute in vivo injury, we used our 5′-bromo-2′-deoxyuridine (BrdU) 'myofiber birthdating' strategy [20, 37], where BrdU was administered from +1 d to +3 d post injury (dpi) to label regenerated myofibers (Fig. 2C). Quantification of total CNFs (Fig. 2D, E) and BrdU-labeled CNFs (Fig. 2D, F), showed that compared to acutely-injured juvenile D2-WT, regeneration was greatly enhanced in adult D2-WT, mirroring results following spontaneous injury in D2-*mdx* (Fig. 2A, B). Nearly 60% of all the myofibers in adult D2-WT muscles were regenerated (CNFs), which was not different from the level of CNFs in B10-WT adult muscle but roughly 3-times greater than in juvenile D2-WT (Fig. 2D, E). The number of CNFs mirrored the extent of BrdU-labeled myofibers over the 2 dpi interval, again revealing a similar trend—greater regeneration in adult D2-WT muscles comparable with adult B10-WT. Meanwhile, juvenile D2-WT showed only minor (<5%) BrdU-labeling in randomly dispersed, small-caliber myofibers that constituted large areas of unresolved inflammation even after 6 dpi (Fig. 2D, F). Overall, we observed that compared to juvenile D2-WT, there is a

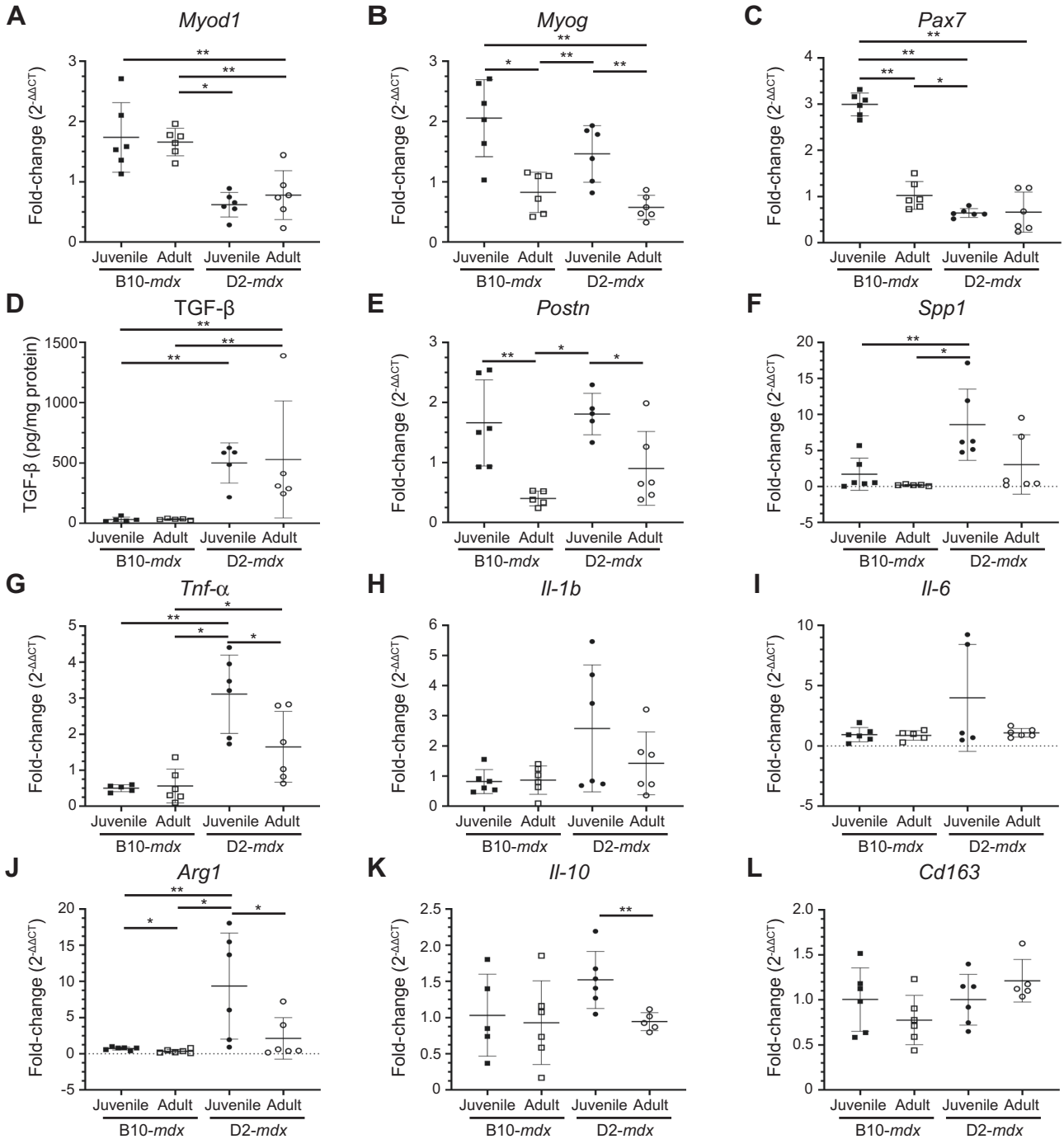

Fig. 3 Expression of genes indicative of myogenesis, ECM, and inflammation in juvenile and adult mouse muscles. A–**C** Gene expression analysis of myogenic markers, *MyoD*, *MyoG*, and *Pax7* in juvenile (5.5 ± 1.5 wk) and adult (8.5 ± 1.5 mo) D2-*mdx* and B10-*mdx* triceps. **D** Levels of active TGF-β protein assessed by ELISA from juvenile and adult D2-*mdx* and B10-*mdx* triceps. **E**, **F** Gene expression analysis of ECM remodeling markers, *Postn* and *Spp1*, in juvenile and adult D2-*mdx* and B10-*mdx* triceps. **G**–**L** Gene expression analysis of inflammatory genes associated with pro-inflammatory (*Tnf-α*, *Il-1b*, *Il-6*) and pro-regenerative (*Arg1*, *Il-10*, *Cd163*) macrophage phenotypes in juvenile and adult D2-*mdx* and B10-*mdx* triceps. Data represent mean ± SD from $n = 5$–6 mice per cohort. *$p < 0.05$, **$p < 0.01$ by Mann–Whitney test.

greatly improved regenerative response in adult D2-WT muscles (Fig. 2).

Stromal alterations mark the regenerative deficit of juvenile D2-mdx muscles

Skeletal muscle regeneration is a multicellular response where SCs interact with the ECM, macrophages, and FAPs to regulate SC proliferation, differentiation, and fusion. To assess the involvement of SC, macrophage, or FAP dysregulation in the regenerative deficit observed in the juvenile D2-*mdx* muscles, we examined the expression of genes associated with these different cell types in triceps (Fig. 3). Analysis of the activated SC marker—myoblast determination protein 1 (*MyoD*), showed that the robust regeneration observed in B10-*mdx* muscle, was associated with higher levels of *MyoD* transcript, while the increased damage and regeneration in juvenile (as compared to an adult) *mdx* mouse

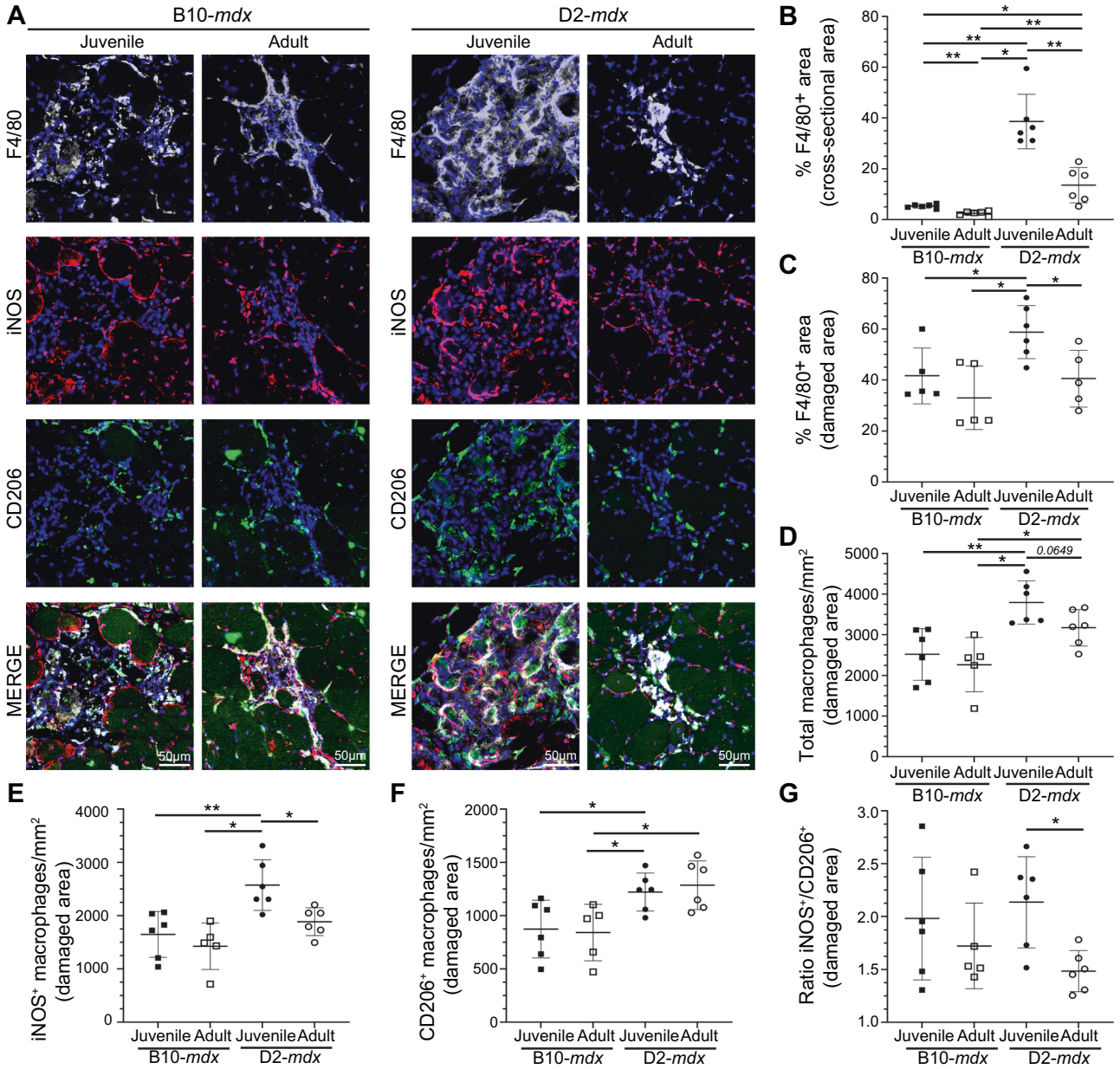

Fig. 4 Investigation of macrophage response to spontaneous injury in *mdx* muscles. A Images showing juvenile (5.5 ± 1.5 wk) and adult (8.5 ± 1.5 mo) D2-*mdx* and B10-*mdx* triceps muscle cross-sections stained to mark F4/80, iNOS, and CD206 expressing macrophages. **B**, **C**. Quantification of F4/80$^+$ area (%) per total cross-sectional area (**B**) and only in damaged areas (areas with abundant F4/80$^+$ macrophage infiltration) within cross-sections (**C**) in juvenile and adult D2-*mdx* and B10-*mdx* triceps. **D** Total macrophages per unit area (mm^2) within damaged regions of juvenile and adult D2-*mdx* and B10-*mdx* triceps cross-sections. **E**–**G** Quantification of the distribution of pro-inflammatory (iNOS$^+$/F4/80$^+$) (**E**), and pro-regenerative (CD206$^+$/F4/80$^+$) (**F**) macrophages, and the ratio of these macrophages (**G**) within damaged areas of triceps muscles from juvenile and adult D2-*mdx* and B10-*mdx*. Data represent mean ± SD from $n = 6$ mice per cohort. *$p < 0.05$, **$p < 0.01$ by Mann–Whitney test.

muscle, was associated with higher myogenin (*MyoG*) transcript in these muscles (Fig. 3A, B). To assess whether improvements in regeneration in adult D2-*mdx* were a consequence of increased SCs, we monitored total levels of Paired Box 7 (*Pax7*) transcript; however, we observed no consistent strain- or age-specific difference for Pax7 transcript (Fig. 3C).

Next, we examined FAP/ECM-related markers and their dynamics with age and disease progression. TGF-β serves as a master modulator of ECM remodeling and composition during muscle repair and we previously demonstrated its heightened activity in juvenile D2-*mdx* at disease onset [20]. We observed higher TGF-β protein activity in the D2-*mdx* as compared to B10-*mdx*, however, the TGF-β activity levels did not change between juvenile and adult D2-*mdx* (Fig. 3D). Due to the extensive effects TGF-β exerts on the regulatory and structural components of the ECM, we next assessed the expression of TGF-β responsive matrix components implicated in dystrophic muscle pathogenesis. Periostin (*Postn*) is a fibroblast-secreted ECM regulatory and structural component whose activity is linked with fibrosis and myogenic function in dystrophic muscle [38]. Like *MyoG*, greater muscle damage seen in juvenile mice was associated with greater levels of periostin (*Postn*), and this was the same in both D2-*mdx* and B10-*mdx* (Fig. 3E). Osteopontin (*Spp1*), a known genetic

modifier in DMD patients, functions to influence ECM architecture and fibrosis, while *Spp1* ablation improves muscle function and influences ECM and macrophage polarization [39–43]. In contrast to *Postn*, *Spp1* was upregulated in juvenile D2-*mdx* compared to adult D2-*mdx*, but this was not the case between B10-*mdx* cohorts (Fig. 3F). This suggests that low expression of *Spp1* in adult D2-*mdx* may improve regenerative capacity by regulating macrophage polarization [40, 41].

Examination of markers of macrophage activity and polarization in B10-*mdx* and D2-*mdx* muscles identified a consistent upregulation of both pro-inflammatory and pro-regenerative macrophage markers in juvenile D2-*mdx* muscles. In terms of pro-inflammatory macrophage markers, while Tumor necrosis factor alpha (*Tnf-α*) was significantly altered between juvenile and adult D2-*mdx*, Interleukin 1b (*Il-1b*) and Interleukin 6 (*Il-6*) exhibited a trend for elevated expression in juvenile D2-*mdx* (Fig. 3G–I). However, the increase tended to be lower in the adult D2-*mdx* muscles and was comparable to the adult B10-*mdx* muscles (Fig. 3G–I). Similarly, markers of pro-regenerative macrophages, specifically Arginase 1 (*Arg1*), and Interleukin-10 (*Il-10*), but not Cluster of differentiation 163 (*Cd163*), were significantly increased in juvenile D2-*mdx* compared to adult D2-*mdx* (Fig. 3J–L).

Thus, while we observed no consistent change in SC and ECM markers between the juvenile and adult D2-*mdx* or between the juvenile and adult B10-*mdx*, we observe consistent dysregulation of *Spp1*, and inflammatory markers corresponding to both pro-inflammatory and pro-regenerative macrophages in juvenile D2-*mdx* muscle as compared to B10-*mdx* and adult D2-*mdx* (Fig. 3F–I). This implicates changes in the muscle inflammatory niche in the poor myogenic response specific to juvenile D2-*mdx* muscles. Analysis of the local muscle niche requires spatial exploration of the inflammatory response to monitoring the histologically defined damaged regions of the muscle [44].

Regenerative deficit of juvenile D2-mdx is linked to a heightened pro-inflammatory response

The dynamic interplay between pro-inflammatory and pro-regenerative macrophages is critical for the timely resolution and repair of muscle tissue. To examine the inflammatory

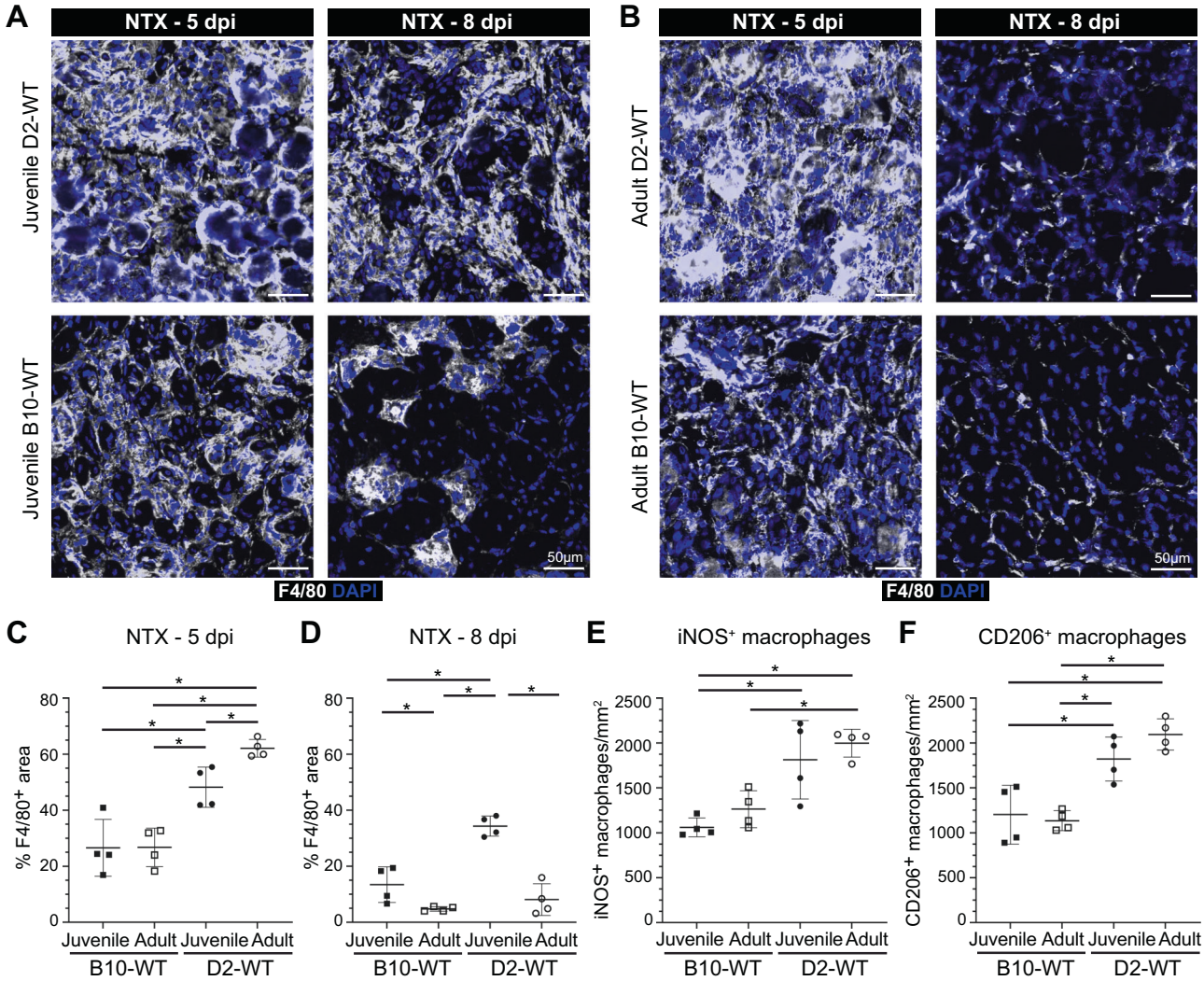

Fig. 5 Investigating dynamics of macrophage inflammatory response after acute injury of healthy muscle. A, **B** F4/80 expression assessed 5 d or 8 d post-injury (dpi) in TA muscles of juvenile (5.5 ± 1.5 wk) and adult (10.5 mo) D2-WT and B10-WT mice. IF images of muscle sections stained to show the distribution of macrophages (F4/80) in adult B10-WT and D2-WT NTX-injured TA muscles after 5 d and 8 d post-injury; muscles co-stained with DAPI. **C**, **D** Quantification of F4/80$^+$ area after NTX-injury assessed 5 dpi (**C**) and 8 dpi (**D**) in juvenile B10-WT and D2-WT. **E**, **F** Quantification of the distribution of pro-inflammatory (iNOS$^+$, F4/80$^+$) (**E**) and pro-regenerative (CD206$^+$, F4/80$^+$) (**F**) macrophages per damaged area (mm^2) in B10-WT and D2-WT NTX-injured TA muscles. Data represent mean ± SD from $n = 4$ mice per cohort. *$p < 0.05$, **$p < 0.01$ by Mann–Whitney test.

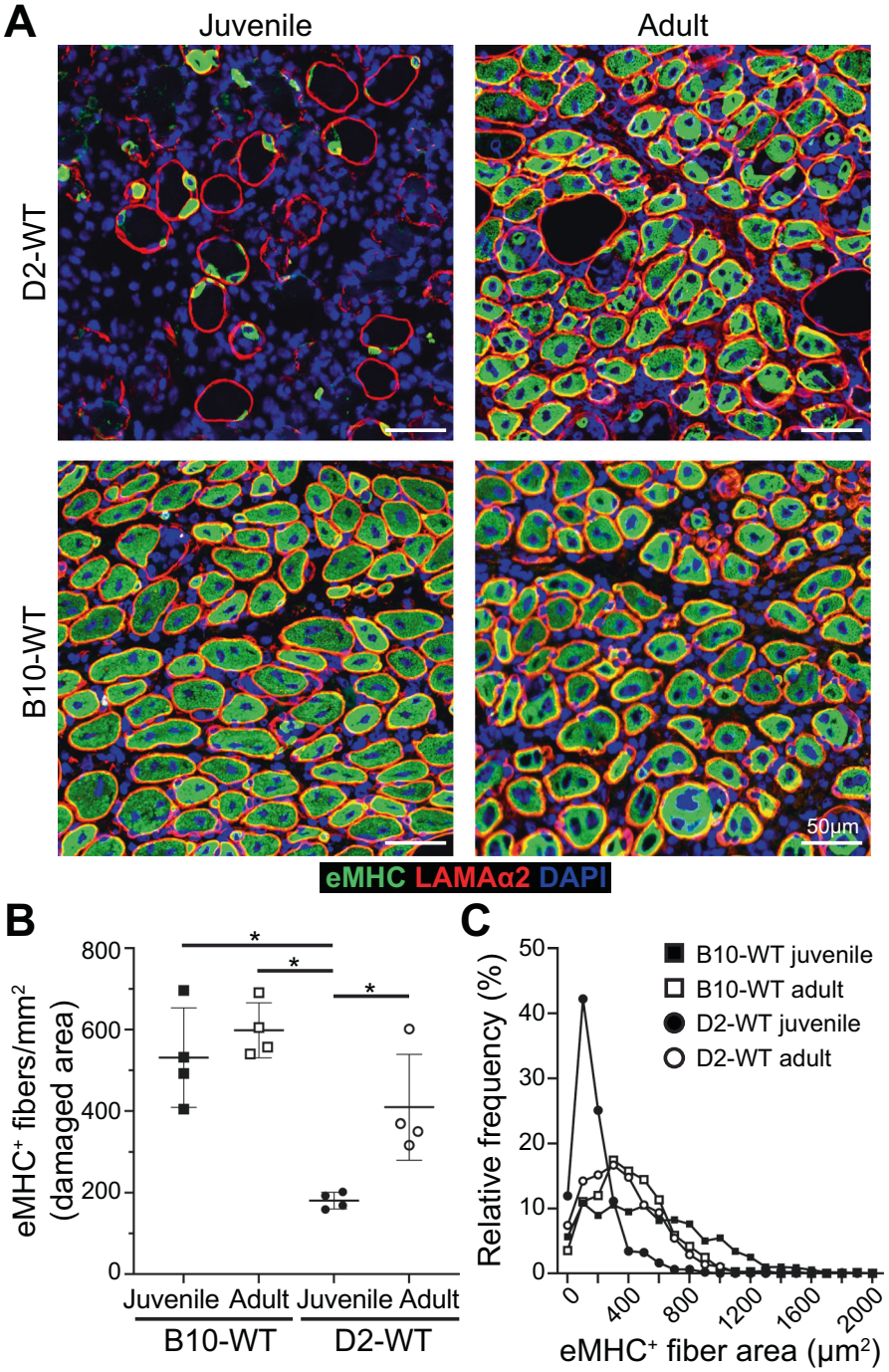

Fig. 6 Investigating regenerative response after acute injury of healthy muscle. A eMHC expression assessed 5 d post-injury (dpi) in TA muscles of juvenile (5.5 ± 1.5 wk) and adult (10.5 mo) D2-WT and B10-WT mice. IF images show the distribution and size of regenerated, eMHC$^+$ myofibers (green), co-stained with Laminin-α2 (red) and DAPI. **B** Quantification of eMHC$^+$ myofibers per mm^2 of damaged tissue present 5 dpi in juvenile and adult D2-WT and B10-WT TA muscles. Data represent mean ± SD from $n = 4$ mice per cohort. *$p < 0.05$ by Mann–Whitney test. **C** Relative frequency plot of eMHC$^+$ myofiber area (reported in μm^2) at 5 dpi in juvenile and adult D2-WT and B10-WT TA muscles, where fiber area was quantified for 1119 fibers (B10-WT juvenile), 496 fibers (D2-WT juvenile), 829 fibers (B10-WT adult), and 866 fibers (D2-WT adult).

response to spontaneous injury of *mdx* muscle we used the pan macrophage marker, F4/80, in conjunction with pro-inflammatory (iNOS) and pro-regenerative (CD206) macrophage markers, and quantified the proportions of pro-inflammatory and pro-regenerative macrophages at and away from the sites of muscle damage (Fig. 4). F4/80 immunostaining shows widespread macrophage infiltration in juvenile D2-*mdx* muscle, which is decreased by more than half in muscles from adult D2-*mdx* (Fig. 4A, B). Focusing exclusively on the damaged areas characterized by the presence of interstitial mononuclear cells, damaged myofibers, and appearance of small-diameter CNFs, we observed a greater abundance of macrophages resulting in a greater density of F4/80 lbeling per unit damaged area in juvenile D2-*mdx* (Fig. 4C).

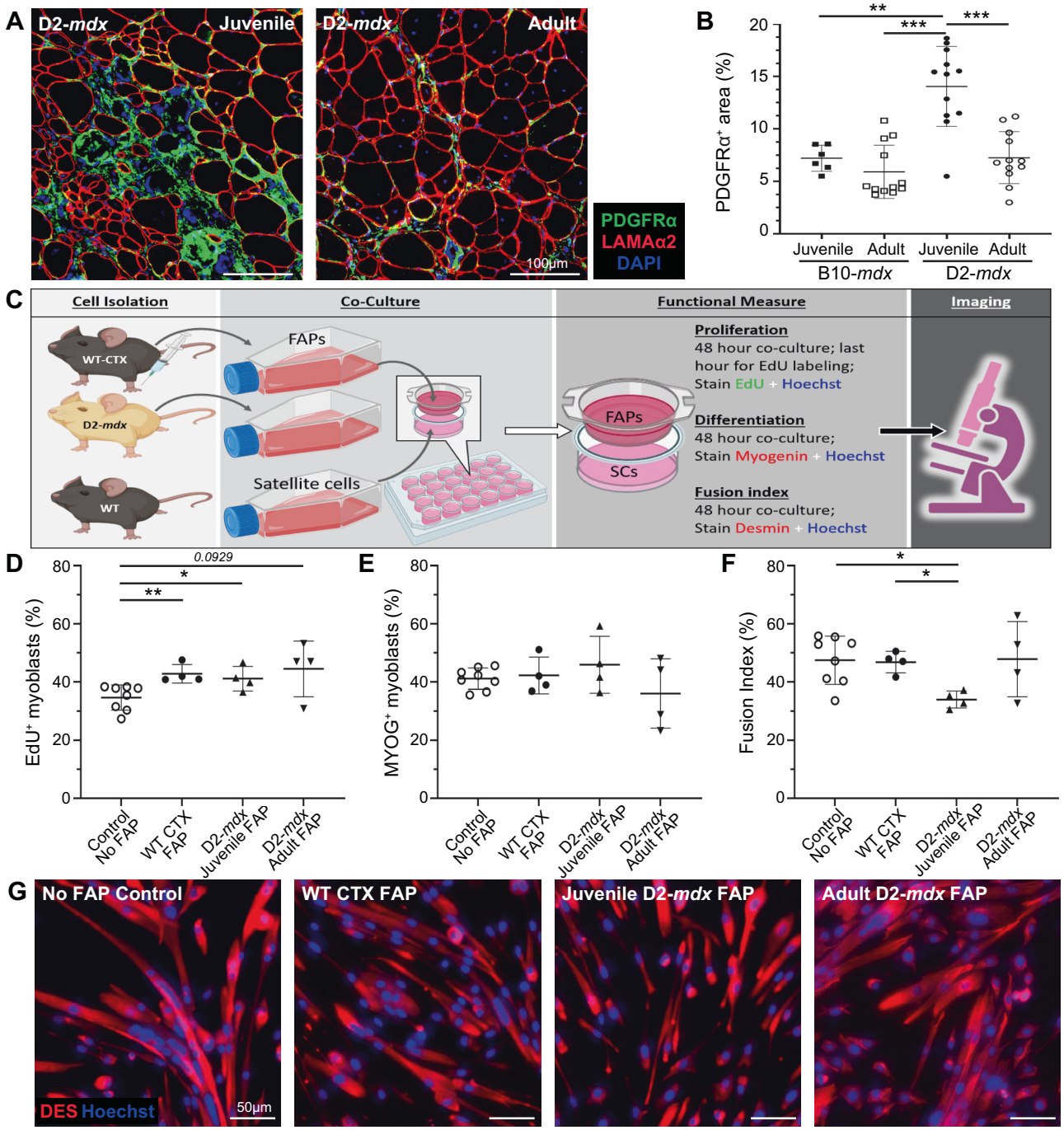

Fig. 7 Analysis of juvenile D2-*mdx* FAPs on satellite cell function. A, **B** IF images and quantification of PDGFRα$^+$ FAPs in juvenile and adult D2-*mdx* and B10-*mdx* triceps immunostained for (Laminin-α2), PDGFRα (green), and interstitial nuclei (DAPI). **C** Schematic illustrating the approach for co-culture experiments to evaluate the effect of FAPs on functional properties of healthy SCs. SCs from uninjured B6-WT mice were co-cultured with FAPs isolated from B6-WT mice at 4 d post cardiotoxin (CTX) injury (WT CTX, 7 wk), juvenile D2-*mdx* (7 wk) mice, or adult D2-*mdx* (5.5 mo) mice. **D** Quantification of the SC proliferation monitored by EdU incorporation. **E** Quantification of the SC differentiation monitored by Myogenin expression. **F**, **G** Quantification of the SC fusion index (**F**) monitored by staining for Desmin (DES) expression with corresponding IF images (**G**) (Desmin– red, Hoechst—blue). Data represent mean ± SD from $n = 6$–12 mice per cohort (**A**, **B**) or $n = 4$–6 individual replicates carried out for each functional measure (**C**–**G**). *$p < 0.05$, **$p < 0.01$, ***$p < 0.001$, by Mann–Whitney test.

As F4/80 does not distinguish between pro-inflammatory and pro-regenerative macrophages, we next evaluated the contribution of these macrophage subtypes to the total macrophage response observed in juvenile D2-*mdx* by co-labeling tissue sections for iNOS$^+$, F4/80$^+$ pro-inflammatory, and CD206$^+$, F4/80$^+$ pro-regenerative macrophages (Fig. 4A). The sum total of each of these macrophage types in damaged areas corresponded to our finding with (F4/80$^+$) macrophage labeling in juvenile D2-*mdx* muscle. Here we observed the highest macrophage density per unit damaged area, which was reduced in adult D2-*mdx* muscles (Fig. 4D). Monitoring individual macrophage populations revealed that the damaged areas of the juvenile D2-*mdx* muscles were enriched in iNOS$^+$ and CD206$^+$ macrophages. In the adult D2-*mdx* muscle, these pro-inflammatory macrophages in areas of damaged

muscle had returned to levels comparable to B10-*mdx*, while the level of pro-regenerative CD206$^+$ macrophages remained elevated (Fig. 4E, F). Examination of the relative proportion of pro-inflammatory to pro-regenerative macrophages (iNOS$^+$/CD206$^+$ macrophages), showed that, inflammation in the juvenile D2-*mdx* muscles, relative to adult D2-*mdx* muscle, is skewed towards the pro-inflammatory status (Fig. 4G). Together, these analyses indicate that juvenile D2-*mdx* muscles are abnormally inundated with pro-inflammatory macrophages, which correlates with the poor myogenic capacity of these muscles.

To assess whether the heightened pro-inflammatory response in juvenile D2-*mdx* is on account of increased intravasation or greater retention of inflammatory macrophages, we examined the kinetics of the inflammatory response. As *mdx* muscle suffers from spontaneously-triggered injuries it precludes their use for timed injury experiments. However, as regenerative myogenic deficit is also noted in juvenile D2-WT muscle (Fig. 2E, F), to achieve timed injury we performed acute focal NTX injury to TA muscles of D2-WT and age-matched B10-WT and then compared the resulting inflammatory and myogenic response (Figs. 5, 6). Injury-triggered muscle inflammation progresses from predominantly pro-inflammatory to predominantly pro-regenerative over the week following injury. Thus, we monitored total (F4/80$^+$) macrophages, as well as levels of pro-inflammatory (iNOS$^+$) and pro-regenerative (CD206$^+$) macrophages at both an earlier (5 dpi) and later (8 dpi) time point. F4/80 staining at 5 dpi showed ~2-fold higher levels for juvenile and adult D2-WT than B10-WT counterparts (Fig. 5A–C). This indicated that the muscles of D2-WT mice are predisposed to a stronger inflammatory response irrespective of age, mimicking our observations above in the D2-*mdx* model (Figs. 1–4). Subsequent assessment of the status of the F4/80 response at 8 dpi showed that the inflammation was largely resolved in the juvenile B10-WT and fully resolved in adult B10-WT and D2-WT muscles (Fig. 5A, B, D). In contrast, the extent of inflammation in juvenile D2-WT was much higher than B10-WT, remaining comparable to the levels seen at 5 dpi (Fig. 5A–C). Concomitant with the resolution of inflammation in juvenile B10-WT and adult D2-WT muscles at 8 dpi, we observed regenerating myofibers in the site of injury, which were lacking in the juvenile D2-WT muscle, mirroring our earlier observations (Fig. 2D). Next, we examined the nature of the macrophages in the areas of inflammation in the acutely injured muscles. Our assessments were limited to 5 dpi, as inflammation had resolved by 8 dpi in all cohorts except juvenile D2-WT. We found that both juvenile and adult D2-WT mice mounted a strong inflammatory response that was comparably represented by pro-inflammatory and pro-regenerative macrophages (Fig. 5E, F).

As an independent measure for the formation of nascent myofibers, we stained acutely injured D2-WT and B10-WT TA muscles for embryonic myosin heavy chain (eMHC) and monitored expression 5 dpi in the damaged sites (Fig. 6). This showed widespread eMHC expression in small-caliber CNFs throughout the site of injury in all cohorts except juvenile D2-WT (Fig. 6A, B). The number of eMHC$^+$ fibers in the adult cohort was no different from each other, and the density of eMHC$^+$ fibers in adult D2-WT was comparable to juvenile and adult B10-WT muscles 5 dpi, but eMHC$^+$ fibers were lacking in juvenile D2-WT muscles (Fig. 6A, B). Further, such fibers were notably smaller (< 200 μm^2) and did not fuse together, even when present within the same basement membrane (Fig. 6A, C). Together, these results indicate that D2-WT mice mount a more robust inflammatory response as compared to B10-WT, which fails to resolve in a timely manner in the juvenile D2-WT, leading to the chronic inflammatory response with direct repercussions on regenerative myogenesis.

FAPs isolated from juvenile D2-mdx mice alter satellite cell fusion capacity in vitro

We previously identified FAP dysregulation is associated with a prolonged state of degeneration of D2-*mdx* muscle [20]. Here we examined the role of aberrant stromal response caused by chronic and excessive accumulation of FAPs and inflammatory cells on SC myogenic deficit. We first assessed FAP expansion and numbers during the resolution of spontaneous injury in juvenile D2-*mdx* muscle, by labeling with FAP marker, platelet-derived growth factor receptor-α (PDGFRα) [45]. This revealed nearly 2-fold more FAPs in juvenile D2-*mdx* muscle, as compared to the adult D2-*mdx* or the juvenile/adult B10-*mdx* muscles (Fig. 7A, B). The observation that FAP abundance in adult D2-*mdx* declines to levels seen in B10-*mdx* muscle suggests that the dysregulated FAP response in the juvenile D2-*mdx* muscles may contribute to the myogenic deficit in these muscles.

To investigate whether juvenile D2-*mdx* FAPs impair SC function, we performed co-culture assays and compared the effect of FAPs from juvenile D2-*mdx*, adult D2-*mdx*, and from acutely injured C57BL/6-WT (B6-WT) mice on the proliferation, differentiation, and fusion of B6-WT SCs (Fig. 7C). These SCs were plated in the presence of FAPs isolated from either juvenile D2-*mdx* muscles or adult D2-mdx muscles exhibiting spontaneous muscle injury, or from juvenile B6-WT muscles that were acutely injured by cardiotoxin (CTX) (Fig. 7C–G). Assessment of proliferation rate of WT SCs by 5′-ethynyl-2′-deoxyuridine (EdU) incorporation showed co-culturing with FAPs enhanced SC proliferation, but no difference in proliferation was observed in co-cultures with the different FAPs – CTX-injured B6-WT, juvenile D2-*mdx*, adult D2-*mdx* (Fig. 7D). Next, to examine SC differentiation we quantified the number of myogenin-expressing SCs and found no difference in SC differentiation potential after 48 h when cultured without FAPs or co-cultured with B6-WT, juvenile D2-*mdx*, or adult D2-*mdx* FAPs (Fig. 7E). Finally, we examined fusion capacity of the SCs cultured in the absence of FAPs or in the presence of B6-WT versus D2-*mdx* FAPs harvested from juvenile or adult muscles. This showed a reduction in the fusion index of SCs when co-cultured for 48 h with juvenile D2-*mdx* FAPs, as compared to the no FAP control, CTX-injured B6-WT FAPs, or adult D2-*mdx* FAPs (Fig. 7F, G). This final observation recapitulates the above in vivo observation that 5-dpi juvenile D2-WT muscles have the smallest (<200 μm^2) nascent myofibers that fail to fuse with the adjacent myofibers. Together, these results identify that poor regenerative myogenesis in the juvenile D2 muscles is attributable to a muscle stromal cell niche that inhibits regeneration by inhibiting myotube fusion.

Glucocorticoid treatment improves regenerative myogenesis in injured juvenile D2-WT muscle

To address whether the altered inflammatory and FAP response activated by acute injury is directly responsible for impaired regeneration seen in juvenile D2-*mdx* muscle, we employed the anti-inflammatory glucocorticoid (GC), deflazacort, which is widely prescribed to the DMD patients. As D2-*mdx* mice suffer spontaneous contraction-induced injuries, this precludes the use of the D2-*mdx* model to carry out controlled acute injury studies. However, our results in Fig. 5 show, acute NTX injury of D2-WT muscle recapitulates the aberrant inflammation and myogenic deficit observed in the juvenile D2-*mdx* muscle. Thus, the use of NTX-injured D2-WT muscle is a suitable surrogate to assess the utility of GC treatment to improve regenerative myogenesis in juvenile D2-*mdx* mice. We performed acute focal NTX injury to the TA muscles of D2-WT mice and initiated daily morning dosing with Deflazacort (1 mg/kg) within 24 h of injury and continued for the next 7 d, in conjunction with a 3 d (+1 d to +4 d post NTX) BrdU-labeling protocol (Fig. 8A). Assessment of pro-inflammatory macrophage markers (*Nos2, Il-1b*, and *Il-6*) showed that deflazacort treatment reduced expression of these markers (Fig. 8B–D), while pro-regenerative macrophage marker (*Cd163*) was significantly increased relative to controls (Fig. 8E). This reflected a change in the macrophage polarization and was associated with a reduction in the markers of fibrotic FAPs (*Fn1*, *Col1a1*) in the deflazacort-treated injured muscles (Fig. 8F, G).

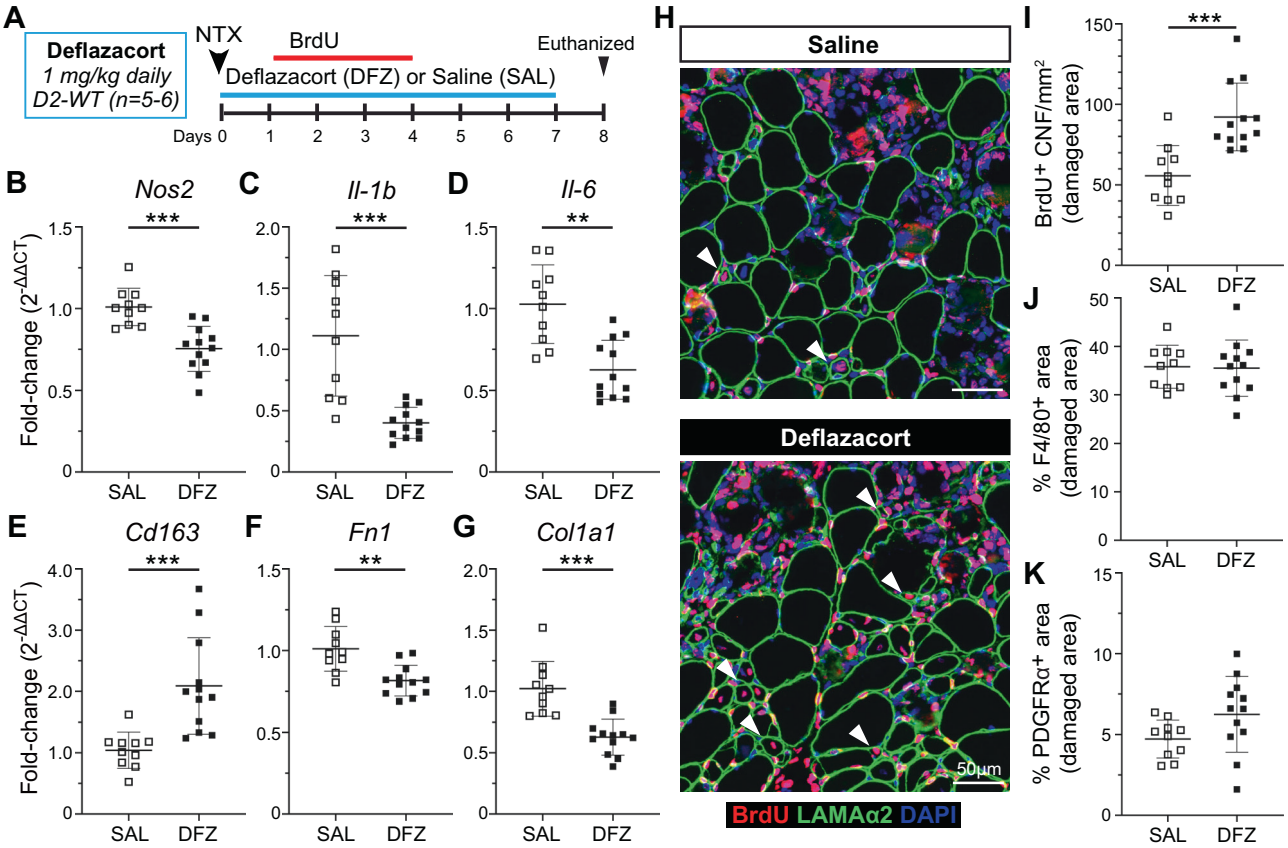

Fig. 8 Analysis of regenerative capacity following acute injury and glucocorticoid treatment. A Schematic showing details for deflazacort treatment regimen performed in juvenile (4–5 wk) D2-WT mice following acute NTX injury. For additional details refer to methods. **B–E** Gene expression analysis of inflammatory genes associated with pro-inflammatory (*Nos2*, *Il-1b*, *Il-6*) and pro-regenerative (*CD163*) macrophage phenotypes in juvenile and adult D2-WT and B10-WT TA muscles after acute injury and deflazacort treatment compared to saline controls. **F, G** Gene expression analysis of ECM markers, *Fn1* and *Col1a1*, in juvenile and adult D2-WT and B10-WT TA muscles after acute injury and deflazacort treatment compared to saline controls. **H** IF images showing BrdU$^+$ CNFs (Red) as indicated by white arrowheads after acute injury and deflazacort treatment compared to saline controls; sections co-stained with Laminin-α2 (green) and DAPI (blue). **I** Quantification of BrdU$^+$ CNFs (per damaged area) after acute injury and deflazacort treatment compared to saline controls. **J, K** % F4/80 (**J**) and PDGFRα (**K**) area reported within damaged muscle regions after acute injury and deflazacort treatment compared to saline controls. Data represent mean ± SD from $n = 5$–6 mice per cohort. $^{**}p < 0.01$, $^{***}p < 0.001$ by Mann–Whitney test.

With improvements in macrophage polarization and fibrotic response of the FAPs, we next assessed if these stromal changes caused by glucocorticoid treatment improved the regenerative capacity of the juvenile D2-WT muscles. Analysis of BrdU-labeled CNFs showed that deflazacort treatment enhanced the myogenic capacity of juvenile D2-WT muscles, leading to a ~1.6-fold increase in the numbers of regenerated myofibers compared to the control (Fig. 8H, I). To evaluate if this improvement in regenerative capacity was the result of reduced macrophage and FAPs within the sites of damage and repair, we also quantified the PDGFRα$^+$ area within the damaged site occupied by macrophages (F4/80$^+$) and FAPs (PDGFRα$^+$) and observed these were no different between deflazacort-treated and control cohorts (Fig. 8J, K). These results indicate the therapeutic potential of glucocorticoid treatment to improve regenerative capacity in juvenile D2-WT muscles by modulating the macrophage polarization and resulting FAP responses such that the niche created by these stromal cell populations in the injured muscle is more conducive to regenerative myogenesis.

DISCUSSION

Poor regenerative capacity contributes to DMD severity by limiting the ability of the muscles to effectively replace damaged myofibers lost due to dystrophin deficiency. Like DMD patients, *mdx* mice are characterized by excessive muscle damage which shows a significant peak during the transition from juvenile to adult stage [46]. Here, we aimed to determine the contribution of poor regenerative ability to progressive muscle loss. In the milder B10-*mdx* mouse model, this acute bout of muscle damage is counteracted by robust regenerative myogenesis, which is lacking in the severe D2-*mdx* model [20]. We show that surprisingly, this myogenic deficit in juvenile D2-*mdx* muscles recovers in adult D2-*mdx*, resulting in a greater proportion of newly regenerated myofibers marked by central nucleation and greater extent of BrdU incorporation during spontaneous bouts of myofiber injury in adult D2-*mdx* muscles than in juvenile D2-*mdx* muscles (Fig. 2). Similar to previous studies [23], we find that the adult D2-*mdx* muscles remain less myogenic than the adult B10-*mdx*. However, the improved myogenic ability of the adult D2-*mdx* helps to explain the previous report of amelioration of disease pathology with age in the D2-*mdx* model [21]. It also explains our observation that the extent of muscle damage in adult D2-*mdx* mice is comparable to the less severe B10-*mdx* model (Fig. 1).

Disturbances of asymmetric cell division and SC depletion in older individuals have been described as intrinsic impairments in SC that compromise the regeneration of the dystrophic muscles

[47]. However, we find that the improved regenerative myogenesis of the adult D2-*mdx* muscle occurs despite no depletion of SCs in juvenile muscles (indicated by SC-specific markers, Pax7 and MyoD), as compared to adult D2-*mdx* muscle. Concomitantly, expression of myogenin (an indicator of myogenic differentiation) is comparable between the mild (B10-*mdx*) and the severe (D2-*mdx*) models (Fig. 3). These findings agree with prior work showing comparable SC pools and myogenic activity between dystrophic and WT muscles [48, 49]. Based on in vivo SC transplant and in vitro analysis of stromal interaction with SCs, it is clear that the muscle niche also plays an important role in SC-mediated regenerative myogenesis [16, 35, 50, 51]. In support of the role played by SC extrinsic factors (muscle niche) in the regulation of regenerative myogenesis, we observed that higher expression of ECM and inflammatory regulators including *Spp1*, *Arg1*, *Tnf-a*, *Il-10* is robustly aligned with the regenerative failure observed in the juvenile D2-*mdx* muscle (Fig. 3). A recent single cell and spatial transcriptomic study identified expansion of a unique pro-inflammatory macrophage subcluster within *mdx* dystrophic lesions that modulates FAP activity and fibrosis through *Spp1* [44]. Interestingly this pathogenic immune-stromal cell interaction is conserved amongst other chronic inflammatory myopathies, including DMD [44].

Analyses of muscle ECM and inflammatory regulators have established the importance of these factors in regulating SC quiescence, activation, and myogenic differentiation [32, 52]. ECM components and stromal cell response to injury have been observed to be altered in the D2-*mdx* model [19, 20]. In agreement with these changes, we observed a distinct inflammatory response to a muscle injury in the D2 (WT and *mdx*) models, such that juvenile *D2-mdx* muscles exhibit a stronger inflammatory response to injury (Fig. 4). In adult *D2-mdx* muscle, the inflammatory response is restored to levels comparable to B10-*mdx*, implicating the excessive inflammatory response in myogenic deficit seen in the juvenile D2-*mdx* mice. Analysis of timed muscle injury in D2-WT mice showed that the excessive inflammatory response to a muscle injury in the juvenile D2-WT mice is caused by delayed clearance of inflammatory macrophages that intravasate into the injured tissue (Fig. 5), adopting a state that hinders regeneration of these inflamed lesions (Fig. 6). Such aberrant clearance of inflammatory cells is a hallmark of asynchronous regeneration and was previously implicated in excessive fibrosis and failed regeneration in *mdx* and DMD patient muscles [8, 34]. Concomitant with the co-occurrence of altered ECM and inflammatory responses, we previously demonstrated increased FAP accumulation in the damaged areas of *D2-mdx* muscles, where aberrant FAP responses are inhibitory to regenerative myogenesis [20, 53, 54]. We found that the aberrant stromal (ECM and inflammatory) response alters FAP activity in the juvenile D2-*mdx* such that even in an ex vivo co-culture assay, these FAPs significantly suppressed SC-mediated regenerative myogenesis. Our analysis determined that it is not the proliferation or differentiation of SCs, but the stage of SC fusion that is diminished selectively by the FAPs derived from the juvenile *D2-mdx* but not from the injured WT muscles or adult D2-*mdx* muscles (Fig. 7). In support of this, we observed that treatment of injured muscles in juvenile D2-WT mice with deflazacort inhibits the aberrant inflammatory and fibrotic response and improves the stromal cell niche that is more supportive of regenerative myogenesis (Fig. 8).

These studies identify the aberrant muscle niche as the driver for the myogenic deficit in the juvenile *D2-mdx* model, which is attenuated by maturation and restoration of the stromal niche in adult *D2-mdx* muscles, resulting in improved regenerative myogenesis in adult mice. This finding suggests targeting the extracellular response to injury as an attractive target to reduce myogenic deficit and severity of disease in DMD.

MATERIALS AND METHODS

Animals

All animal protocols were reviewed and approved by the Institutional Animal Care and Use Committee (IACUC) of the Children's National Research Institute and Institut NeuroMyoGène. Male and female mice were used and grouped into specific cohorts based on their age—juvenile 5.5 ± 1.5 wk old, and adult 8.0 ± 2.5 mo old. Mice were maintained under normal, ambient conditions with continuous access to food/water until they were euthanized by CO_2 and cervical dislocation. Tissues were harvested, frozen, and stored at −80 °C. For in vivo studies, we used dystrophic mouse models harboring a point mutation in Dmd exon 23, C57BL/10ScSn-mdx/J (B10-*mdx*) and DBA/2J-*mdx* (D2-*mdx*) mice, as well as their corresponding genotype controls – C57BL/10ScSnJ (B10-WT) and DBA/2 J (D2-WT). For in vitro culture studies, primary FAPs were harvested from CTX-injured C57BL/6-WT (B6-WT), or from juvenile or adult D2-*mdx* mice. As SC from D2 mice exhibit an intrinsic deficit in their myogenic ability [24], healthy SCs were obtained and harvested from B6-WT mice based on our prior finding that C57BL/6 and C57BL/B10 muscles exhibit similar myogenesis [20]. For each experiment, mice were randomized based on sex and body weight, and outcomes were analyzed in an unblinded manner through independent assessment by more than one investigator. All mice were originally obtained from The Jackson Laboratory and bred in-house for all experiments.

BrdU labeling

5′-bromo-2′-deoxy-uridine (BrdU) (Sigma-Aldrich, B9285) was administered ad libitum in drinking water (0.8 mg/mL) and kept protected from light during administration [20, 37]. Mice received BrdU ad libitum in drinking water for the designated period of time indicated in each experiment following spontaneous or NTX-induced injury. Mice were subsequently euthanized, and tissues were harvested for processing 3 d after cessation of BrdU administration [20].

Toxin-induced injury

Animals were anesthetized with isoflurane and the anterior hind limb was shaved before intramuscular injection of notexin (NTX) or cardiotoxin (CTX) as previously described [20, 34, 55].

Deflazacort treatment

Deflazacort (1 mg/kg, daily, I.P., Sigma-Aldrich, 1166116) was administered to D2-WT mice (4 wk) within 24 h following NTX injury and continued daily at 11 am (±1 h; light-cycle dosing schedule) for a period of 7 d. Control D2-WT mice were administered saline. Mice received BrdU ad libitum in drinking water from 24 to 72 h after NTX (refer to Fig. 8A).

Histology and immunofluorescence

Frozen muscles were sectioned at 8 µm thickness using a Leica CM1950 cryostat chilled to −20 °C, where tissues were mounted on slides and stained using Hematoxylin and Eosin (H&E), Alizarin Red, and Masson's Trichrome according to TREAT-NMD Standard Operating Procedures for quantification of damage, calcification, and fibrosis, respectively, as previously described [20], or for immunostaining procedures as previously described [20, 37]. For measures of pathology (fibrosis, damage, and calcification) and regeneration (% CNF and % $Brdu^+$ CNF), quantification was performed across the entire muscle cross-section for each tissue sample. Muscle sections were stained with primary and secondary antibodies as described in Supplementary Table 1.

Microscopy

We used Olympus VS120-S5 Virtual Slide Scanning System with UPlanSApo 40×/0.95 objective, Olympus XM10 monochrome camera, and Olympus VS-ASW FL 2.7 imaging software. Analysis was performed using Olympus CellSens 1.13 and ImageJ software.

Gene expression

Triceps muscles were used to perform gene expression analysis. Total RNA was extracted from muscle samples by standard TRIzol (Life Technologies) isolation. Purified RNA (400 ng) was reverse-transcribed using Random Hexamers and High-Capacity cDNA Reverse Transcription Kit (Thermo Fisher, 4368814). The mRNAs were quantified using individual TaqMan assays described in Supplementary Table 2 on an ABI QuantStudio 7 Real-

Time PCR machine (Applied Biosystems) using TaqMan Fast Advanced Master Mix (Thermo Fisher, 4444556).

TGF-β1 ELISA

Levels of active TGF-β1 in triceps were quantified using Quantikine ELISA mouse TGF-β1 immunoassay (R&D Systems, MB100B) according to the manufacturer's recommendations and as previously described [20]. Final values were normalized to total protein concentration.

Isolation of satellite cells and FAPs

SCs were isolated from the hindlimb muscles of C57BL/6 mice ($n = 4$–6) using negative selection MACS Satellite Cell Isolation Kit (Miltenyi, 130-104-268) according to the manufacturer's protocols. Muscles were minced and incubated with Muscle Dissociation Buffer (Ham's F-10 (Sigma, N6908), 5% horse serum (Gibco, 16050-130), 1% penicillin/streptomycin (P/S) (Gibco, 15140-122), collagenase II (Gibco, 17101-105)) at 37 °C for 60 min with agitation (60–70 RPM). Suspensions were re-incubated with collagenase II and dispase (Gibco, 17105-041) in Ham's F-10 supplemented with 5% Horse Serum and 1% P/S at 37 °C with agitation for 30 min. Suspensions were filtered and the MACS LS column was sorted (Miltenyi, 130-042-401). Cells were re-suspended in DMEM F-12 (Gibco, 31331-028) supplemented with 20% FBS (Gibco, 10270-106), 2% Ultroser G (Pall Gelman Sciences, 15950-017), and 1% P/S. As CTX injury of mouse muscle leads to SCs that are comparable in numbers and properties to those isolated following NTX injury [55], we interchangeably used CTX injury to isolate FAP and SCs for culture studies. FAPs were isolated from gastrocnemius muscles of n = 4-6 juvenile (7 wk) B6-WT 4 d post-CTX injury, juvenile (7 wk) D2-*mdx*, or adult (5.5 mo) D2-*mdx* by pre-plating the cell suspension for 4 h after the digestion procedure described above. Cells were washed with PBS and left to amplify in non-coated flasks for 4–5 days in a growth medium (DMEM F-12, 10% FBS, 1% P/S).

Co-culture of satellite cells and FAPs

SCs isolated from B6-WT mice and FAPs isolated from CTX-injured B6-WT, or uninjured juvenile or adult D2-*mdx* muscles, were co-cultured without FAPs (No FAP) or FAPs isolated from indicated WT or *mdx* mice cultured on 0.4 µm porous transwell culture inserts (Nunc, 056408). SCs were plated in the bottom of the transwell coated with HGF Matrigel (BD Biosciences, 354234), while FAPs were plated in the upper insert. SCs and FAPs were plated in a 1:3 ratio in a low serum growth medium (DMEM, 2.5% FBS, 1% P/S) and assays were performed after 48 h. For proliferation assay, SCs were plated at 2000 cells/cm^2, and EdU incorporation was performed after 48 h and detected using Click-iT™ EdU Cell Proliferation Kit (Thermo Fisher, C10337). For differentiation assay, SCs were plated at 10,000 cells/cm^2, and myogenin (Santa Cruz, SC-12732) staining was used to evaluate differentiation. For the fusion assay, SC was plated at 50,000 cells/cm^2, and desmin (Abcam, ab32362) staining was performed to quantify the fusion index. RAW data acquired from different experiments were normalized to no FAP controls.

Statistics

Sample size estimations were based on a similar study we previously performed [20]. GraphPad Prism 9.2.0 was used for all statistical analyses of data. Statistical analysis was performed using the non-parametric Mann–Whitney test. Data normality was assessed for all statistical comparisons. All *p*-values less than 0.05 were considered statistically significant; $*p < 0.05$, $**p < 0.01$, $***p < 0.001$, and $****p < 0.0001$. Data plots were reported as scatter plots with mean ± SD.

DATA AVAILABILITY

All data will be made promptly available to the scientific community upon request.

REFERENCES

1. Hoffman EP, Brown RH Jr, Kunkel LM. Dystrophin: the protein product of the Duchenne muscular dystrophy locus. Cell. 1987;51:919–28.
2. Mendell JR, Shilling C, Leslie ND, Flanigan KM, al-Dahhak R, Gastier-Foster J, et al. Evidence-based path to newborn screening for Duchenne muscular dystrophy. Ann Neurol. 2012;71:304–13.
3. Ibraghimov-Beskrovnaya O, Ervasti JM, Leveille CJ, Slaughter CA, Sernett SW, Campbell KP. Primary structure of dystrophin-associated glycoproteins linking dystrophin to the extracellular matrix. Nature. 1992;355:696–702.
4. Allikian MJ, McNally EM. Processing and assembly of the dystrophin glycoprotein complex. Traffic. 2007;8:177–83.
5. Petrof BJ, Shrager JB, Stedman HH, Kelly AM, Sweeney HL. Dystrophin protects the sarcolemma from stresses developed during muscle contraction. Proc Natl Acad Sci USA. 1993;90:3710–4.
6. Petrof BJ. The molecular basis of activity-induced muscle injury in Duchenne muscular dystrophy. Mol Cell Biochem. 1998;179:111–23.
7. Vila MC, Rayavarapu S, Hogarth MW, Van der Meulen JH, Horn A, Defour A, et al. Mitochondria mediate cell membrane repair and contribute to Duchenne muscular dystrophy. Cell Death Differ. 2017;24:330–42.
8. Dadgar S, Wang Z, Johnston H, Kesari A, Nagaraju K, Chen YW, et al. Asynchronous remodeling is a driver of failed regeneration in Duchenne muscular dystrophy. J Cell Biol. 2014;207:139–58.
9. Chen YW, Nagaraju K, Bakay M, McIntyre O, Rawat R, Shi R, et al. Early onset of inflammation and later involvement of TGFbeta in Duchenne muscular dystrophy. Neurology. 2005;65:826–34.
10. Kharraz Y, Guerra J, Pessina P, Serrano AL, Munoz-Canoves P. Understanding the process of fibrosis in Duchenne muscular dystrophy. BioMed Res Int. 2014;2014:965631.
11. Cros D, Harnden P, Pellissier JF, Serratrice G. Muscle hypertrophy in Duchenne muscular dystrophy. A pathological and morphometric study. J Neurol. 1989;236:43–47.
12. Webster C, Blau HM. Accelerated age-related decline in replicative life-span of Duchenne muscular dystrophy myoblasts: implications for cell and gene therapy. Somat Cell Mol Genet. 1990;16:557–65.
13. Blau HM, Webster C, Pavlath GK. Defective myoblasts identified in Duchenne muscular dystrophy. Proc Natl Acad Sci USA. 1983;80:4856–60.
14. Decary S, Hamida CB, Mouly V, Barbet JP, Hentati F, Butler-Browne GS. Shorter telomeres in dystrophic muscle consistent with extensive regeneration in young children. Neuromuscul Disord. 2000;10:113–20.
15. Kharraz Y, Guerra J, Mann CJ, Serrano AL, Munoz-Canoves P. Macrophage plasticity and the role of inflammation in skeletal muscle repair. Mediat Inflamm. 2013;2013:491497.
16. Saclier M, Cuvellier S, Magnan M, Mounier R, Chazaud B. Monocyte/macrophage interactions with myogenic precursor cells during skeletal muscle regeneration. FEBS J. 2013;280:4118–30.
17. Pascual-Morena C, Cavero-Redondo I, Saz-Lara A, Sequi-Dominguez I, Luceron-Lucas-Torres M, Martinez-Vizcaino V. Genetic modifiers and phenotype of Duchenne muscular dystrophy: a systematic review and meta-analysis. Pharmaceuticals (Basel). 2021;14:798.
18. Flanigan KM, Ceco E, Lamar KM, Kaminoh Y, Dunn DM, Mendell JR, et al. LTBP4 genotype predicts age of ambulatory loss in Duchenne muscular dystrophy. Ann Neurol. 2013;73:481–8.
19. Heydemann A, Ceco E, Lim JE, Hadhazy M, Ryder P, Moran JL, et al. Latent TGF-beta-binding protein 4 modifies muscular dystrophy in mice. J Clin Invest. 2009;119:3703–12.
20. Mazala DA, Novak JS, Hogarth MW, Nearing M, Adusumalli P, Tully CB, et al. TGF-beta-driven muscle degeneration and failed regeneration underlie disease onset in a DMD mouse model. JCI Insight. 2020;5:e135703.
21. van Putten M, Putker K, Overzier M, Adamzek WA, Pasteuning-Vuhman S, Plomp JJ, et al. Natural disease history of the D2-mdx mouse model for Duchenne muscular dystrophy. FASEB J. 2019;33:8110–24.
22. Coley WD, Bogdanik L, Vila MC, Yu Q, Van Der Meulen JH, Rayavarapu S, et al. Effect of genetic background on the dystrophic phenotype in mdx mice. Hum Mol Genet. 2016;25:130–45.
23. Hammers DW, Hart CC, Matheny MK, Wright LA, Armellini M, Barton ER, et al. The D2.mdx mouse as a preclinical model of the skeletal muscle pathology associated with Duchenne muscular dystrophy. Sci Rep. 2020;10:14070.
24. Fukada S, Morikawa D, Yamamoto Y, Yoshida T, Sumie N, Yamaguchi M, et al. Genetic background affects properties of satellite cells and mdx phenotypes. Am J Pathol. 2010;176:2414–24.
25. Olson EN, Sternberg E, Hu JS, Spizz G, Wilcox C. Regulation of myogenic differentiation by type beta transforming growth factor. J Cell Biol. 1986;103:1799–805.
26. Cohn RD, van Erp C, Habashi JP, Soleimani AA, Klein EC, Lisi MT, et al. Angiotensin II type 1 receptor blockade attenuates TGF-beta-induced failure of muscle regeneration in multiple myopathic states. Nat Med. 2007;13:204–10.
27. MacDonald EM, Cohn RD. TGFbeta signaling: its role in fibrosis formation and myopathies. Curr Opin Rheumatol. 2012;24:628–34.
28. Girardi F, Taleb A, Ebrahimi M, Datye A, Gamage DG, Peccate C, et al. TGFbeta signaling curbs cell fusion and muscle regeneration. Nat Commun. 2021;12:750.
29. Contreras O, Cruz-Soca M, Theret M, Soliman H, Tung LW, Groppa E, et al. Cross-talk between TGF-beta and PDGFRalpha signaling pathways regulates the fate of stromal fibro-adipogenic progenitors. J Cell Sci. 2019;132:jcs232157.

30. Lemos DR, Babaeijandaghi F, Low M, Chang CK, Lee ST, Fiore D, et al. Nilotinib reduces muscle fibrosis in chronic muscle injury by promoting TNF-mediated apoptosis of fibro/adipogenic progenitors. Nat Med. 2015;21:786–94.
31. Tidball JG. Regulation of muscle growth and regeneration by the immune system. Nat Rev Immunol. 2017;17:165–78.
32. Morgan J, Partridge T. Skeletal muscle in health and disease. Dis Model Mech. 2020;13:dmm042192.
33. Rosenberg AS, Puig M, Nagaraju K, Hoffman EP, Villalta SA, Rao VA, et al. Immune-mediated pathology in Duchenne muscular dystrophy. Sci Transl Med. 2015;7:299rv294.
34. Juban G, Saclier M, Yacoub-Youssef H, Kernou A, Arnold L, Boisson C, et al. AMPK activation regulates LTBP4-dependent TGF-beta1 secretion by pro-inflammatory macrophages and controls fibrosis in duchenne muscular dystrophy. Cell Rep. 2018;25:2163–2176.e2166.
35. Saclier M, Yacoub-Youssef H, Mackey AL, Arnold L, Ardjoune H, Magnan M, et al. Differentially activated macrophages orchestrate myogenic precursor cell fate during human skeletal muscle regeneration. Stem Cells. 2013;31:384–96.
36. Malecova B, Gatto S, Etxaniz U, Passafaro M, Cortez A, Nicoletti C, et al. Dynamics of cellular states of fibro-adipogenic progenitors during myogenesis and muscular dystrophy. Nat Commun. 2018;9:3670.
37. Novak JS, Hogarth MW, Boehler JF, Nearing M, Vila MC, Heredia R, et al. Myoblasts and macrophages are required for therapeutic morpholino antisense oligonucleotide delivery to dystrophic muscle. Nat Commun. 2017;8:941.
38. Lorts A, Schwanekamp JA, Baudino TA, McNally EM, Molkentin JD. Deletion of periostin reduces muscular dystrophy and fibrosis in mice by modulating the transforming growth factor-beta pathway. Proc Natl Acad Sci USA. 2012;109:10978–83.
39. Vetrone SA, Montecino-Rodriguez E, Kudryashova E, Kramerova I, Hoffman EP, Liu SD, et al. Osteopontin promotes fibrosis in dystrophic mouse muscle by modulating immune cell subsets and intramuscular TGF-beta. J Clin Invest. 2009;119:1583–94.
40. Capote J, Kramerova I, Martinez L, Vetrone S, Barton ER, Sweeney HL, et al. Osteopontin ablation ameliorates muscular dystrophy by shifting macrophages to a pro-regenerative phenotype. J Cell Biol. 2016;213:275–88.
41. Kramerova I, Kumagai-Cresse C, Ermolova N, Mokhonova E, Marinov M, Capote J, et al. Spp1 (osteopontin) promotes TGFbeta processing in fibroblasts of dystrophin-deficient muscles through matrix metalloproteinases. Hum Mol Genet. 2019;28:3431–42.
42. Hirata A, Masuda S, Tamura T, Kai K, Ojima K, Fukase A, et al. Expression profiling of cytokines and related genes in regenerating skeletal muscle after cardiotoxin injection: a role for osteopontin. Am J Pathol. 2003;163:203–15.
43. Bello L, Pegoraro E. The "Usual Suspects": genes for inflammation, fibrosis, regeneration, and muscle strength modify duchenne muscular dystrophy. J Clin Med. 2019; 8.
44. Coulis G, Jaime D, Guerrero-Juarez C, Kastenschmidt JM, Farahat PK, Nguyen Q, et al. Single-cell and spatial transcriptomics identify a macrophage population associated with skeletal muscle fibrosis. Preprint at *bioRxiv*. 2023. https://doi.org/10.1101/2023.04.18.537253.
45. Uapinyoying, Prech and Hogarth, Marshall and Battacharya, Surajit and Mázala, Davi A.G. and Panchapakesan, Karuna and Bonnemann, Carsten and Jaiswal, Jyoti, Single Cell Transcriptomic Analysis of the Identity and Function of Fibro/Adipogenic Progenitors in Healthy and Dystrophic Muscle. iScience; 2023 - in Press.
46. Coulton GR, Morgan JE, Partridge TA, Sloper JC. The mdx mouse skeletal muscle myopathy: I. A histological, morphometric and biochemical investigation. Neuropathol Appl Neurobiol. 1988;14:53–70.
47. Chang NC, Chevalier FP, Rudnicki MA. Satellite cells in muscular dystrophy—lost in polarity. Trends Mol Med. 2016;22:479–96.
48. Boldrin L, Zammit PS, Morgan JE. Satellite cells from dystrophic muscle retain regenerative capacity. Stem Cell Res. 2015;14:20–29.
49. Ribeiro AF Jr, Souza LS, Almeida CF, Ishiba R, Fernandes SA, Guerrieri DA, et al. Muscle satellite cells and impaired late stage regeneration in different murine models for muscular dystrophies. Sci Rep. 2019;9:11842.
50. Meng J, Bencze M, Asfahani R, Muntoni F, Morgan JE. The effect of the muscle environment on the regenerative capacity of human skeletal muscle stem cells. Skelet Muscle. 2015;5:11.
51. Joe AW, Yi L, Natarajan A, Le Grand F, So L, Wang J, et al. Muscle injury activates resident fibro/adipogenic progenitors that facilitate myogenesis. Nat Cell Biol. 2010;12:153–63.
52. Sousa-Victor P, Garcia-Prat L, Munoz-Canoves P. Control of satellite cell function in muscle regeneration and its disruption in ageing. Nat Rev Mol Cell Biol. 2022;23:204–26.
53. Bensalah M, Muraine L, Boulinguiez A, Giordani L, Albert V, Ythier V, et al. A negative feedback loop between fibroadipogenic progenitors and muscle fibres involving endothelin promotes human muscle fibrosis. J Cachexia Sarcopenia Muscle. 2022;13:1771–84.
54. Hogarth MW, Uapinyoying P, Mazala DAG, Jaiswal JK. Pathogenic role and therapeutic potential of fibro-adipogenic progenitors in muscle disease. Trends Mol Med. 2022;28:8–11.
55. Hardy D, Besnard A, Latil M, Jouvion G, Briand D, Thepenier C, et al. Comparative study of injury models for studying muscle regeneration in mice. PLoS ONE. 2016;11:e0147198.

ACKNOWLEDGEMENTS

This work was supported by the National Institutes of Health NIAMS (T32AR056993 | DAGM, JSN, JKJ, and TAP, R01AR055686 | JKJ), the Foundation to Eradicate Duchenne (DAGM, JSN, JKJ), Department of Defense DMDRP (W81XWH2110680 | JKJ; W81XWH2110711 | JSN), The Muscular Dystrophy Association (MD480160, MD970000 | JSN), Children's National Research Institute (CNRI) Institutional Funding (JSN), Towson University College of Health Professions (DAGM), Agence Nationale pour la Recherche (19-CE14-0008-01 | BC) and AFM-Telethon (Alliance MyoNeurALP | BC). Microscopy was performed at the Cell and Tissue Microscopy Core supported by CNRI and The National Institutes of Health NICHD (P50HD105328 | JKJ).

AUTHOR CONTRIBUTIONS

This study was conceived by JSN, TAP, and JKJ. JSN and JKJ designed the experiments with input from DAGM and RH. DAGM, RH, YM, and JSN conducted all in vivo studies, imaging, and molecular analyses; FS, IHG, and DA assisted RH and JSN in histological assessment and quantification. Cell culture assays were performed by GP, MWG, and BC. The manuscript was written by JSN and JKJ, with help from DAGM and RH, and edited by all authors. JSN, BC, and JKJ obtained funding and provided oversight for the pursuit of the study.

COMPETING INTERESTS

The authors declare no competing interests.

ADDITIONAL INFORMATION

Supplementary information The online version contains supplementary material available at https://doi.org/10.1038/s41420-023-01503-0.

Correspondence and requests for materials should be addressed to James S. Novak or Jyoti K. Jaiswal.

Reprints and permission information is available at http://www.nature.com/reprints

Publisher's note Springer Nature remains neutral with regard to jurisdictional claims in published maps and institutional affiliations.